Analyst

Cite this: *Analyst*, 2011, **136**, 2427

www.rsc.org/analyst

CRITICAL REVIEW

Dielectric barrier discharges in analytical chemistry

C. Meyer, S. Müller, E. L. Gurevich and J. Franzke*

Received 13th December 2010, Accepted 12th April 2011
DOI: 10.1039/c0an00994f

The present review reflects the importance of dielectric barrier discharges in analytical chemistry. Special about this discharge is—and in contrast to usual discharges with direct current—that the plasma is separated from one or two electrodes by a dielectric barrier. This gives rise to two main features of the dielectric barrier discharges; it can serve as dissociation and excitation device and as ionization mechanism, respectively. The article portrays the various application fields for dielectric barrier discharges in analytical chemistry, for example the use for elemental detection with optical spectrometry or as ionization source for mass spectrometry. Besides the introduction of different kinds of dielectric barrier discharges used for analytical chemistry from the literature, a clear and concise classification of dielectric barrier discharges into capacitively coupled discharges is provided followed by an overview about the characteristics of a dielectric barrier discharge concerning discharge properties and the ignition mechanism.

Introduction

This review gives an insight into dielectric barrier discharges for analytical application. The term dielectric barrier discharge (DBD) refers to a kind of gas discharge in which plasma is separated from one or two electrodes by a dielectric barrier.

DBDs were first introduced by W. Siemens in 1857 for the purpose of ozone generation in air,[1] although first experiments were held already in 1778 by G. C. Lichtenberg.[2] At the beginning of the 20th century, further research contributed to the understanding of DBD (also referred to as silent discharge). The breakdown of the discharge was characterized by tiny short-lived filaments by photographs and current–voltage records of the microdischarge.[3–5] Since 1970 research activities in modeling and diagnostics were carried out not only resulting in a better understanding of the DBD but also in numerous additional applications. The unique features and characteristics of DBDs offer a wide industrial application including ozone generation mainly used in water and gas treatment, excimer lamps, plasma display panels and surface engineering, *e.g.* cleaning,

ISAS, Dortmund, 44227, Germany. E-mail: franzke@isas.de

Saskia Müller, Cordula Meyer, Evgeny L. Gurevich and Joachim Franzke

Cordula Meyer (2nd from left) obtained her diploma in physics from the Technische Universität (TU) Dortmund, Germany, with a focus on the development of adaptive optical microsystems. She joined the Leibniz-Institut für Analytische Wissenschaften—ISAS—e.V. in 2009 pursuing her PhD degree. Her research focuses on miniaturized plasma based analytical devices and ambient ionization techniques. Saskia Müller (left) received her diploma in physics from TU Dortmund, Germany. Since 2010 she is working at ISAS to obtain her PhD degree with a focus on plasmas for liquid analysis and the characterization of plasmas for ambient ionization techniques. Evgeny L. Gurevich (2nd from right) received his MSc from St Petersburg State University in Russia in 2000. In 2004 he received his PhD in physics from the University of Münster in Germany. From 2004 to 2006 he worked as post-doc at Max-Planck Institute for Dynamics and Self-Organization in Göttingen, Germany. He is currently working at ISAS in Dortmund. His research is focused on pattern formation and laser physics. Joachim Franzke (right) received his PhD in applied plasma spectrometry in 1994 from TU Dortmund. He held positions at the National Institute of Standards and Technology (NIST), Boulder, CO in the group of Leo Hollberg and University of Hohenheim, Germany. Currently, he is head of the miniaturization group at ISAS. His main research interest is the development of analytical methods for the miniaturization of analytical devices, especially the development and characterization of new ionization sources.

aerodynamics drag reduction on moving objects, microwave absorption/reflection, activation and coating deposition.[6–16]

Additionally to these well known industrial applications DBDs make a wide range of analytical applications possible. Regarding analytical chemistry, DBDs provide various advantages. Generally they are easy to set up and operate over a wide pressure range with various discharge gases. The temperature is rather low compared to direct discharges and the dielectric barrier avoids contamination of the analyte sample with electrode material. The power consumption of typically a few watts is low with electron densities up to 10^{15} cm^{-3}. They offer a high rate of dissociation important for element spectroscopy and ionization for molecular spectroscopy.[17] Low power consumption allows making compact cells for miniaturization and lab on a chip applications.[18] Since dielectric barrier discharges are discontinuous having rather a pulsed character with only moderate light intensity (compared to dc discharges), only a few examples of optical spectrometry, especially emission spectrometry, can be found in the literature. Otherwise absorption spectrometry measurements are more promising, reflected by numerous publications. Barrier discharges are further a powerful tool used as ionization source for mass spectrometry or ion mobility spectrometry. Here several analytical examples are given explicitly revealing the wide-ranging benefit of DBDs in manifold operation fields. Besides plasma discharges a unique dielectric barrier discharge in form of an analytical electrospray is presented as well.

This review article begins with a general overview of capacitively coupled plasmas which are divided into discharges at low frequencies in the kHz regime and high frequencies in the MHz regime. For both frequency ranges discharges with and without dielectric layers on the metal electrodes are discussed. A special focus is certainly put on the physical background of the DBD discharge; the ignition mechanism and electrical characteristics are described in detail. The subsequent section reviews various DBD configurations for analytical applications. At first, DBDs for direct elemental detection with optical spectrometry are listed followed by DBDs used as ionization source for mass spectrometric measurements of mostly molecular species. Besides the analytical figures of merit details of the geometrical configuration, excitation voltages and frequencies and the present mechanisms are introduced.

Theoretical background of dielectric barrier discharges

Electric discharges in gases cover a large range of physical effects from lightning till St Elmo's light. Common for all these cases is plasma—a highly ionized gas—produced by ionization processes triggered by an electric field. Hence, the electric field and so the applied voltage is important for characterization. Moreover, the current is decisive. For all types of discharges, mainly two different kinds of currents have to be distinguished. The conduction current caused by an electric field describes charge transfer in conducting media (solids or electrolytes) and is carried by electrons and ions. The displacement current on the other hand is generated by a change in electric field and is not linked to the existence of conducting media. Simply speaking, the charging/discharging current of the capacitor, which is formed by the gas-discharge cell in the dielectric media, contributes to the displacement current according to Ampere's circuital law.

The following section provides an overview of different plasmas to enclose the concept of dielectric barrier discharges. It deals mainly with capacitively coupled plasmas. In this section a classification of DBDs is offered based on the frequency domain of the applied voltage and ignition mechanism.

Plasma can be classified in capacitively coupled plasmas (CCPs) and inductively coupled plasmas (ICP) due to the power input. The latter is briefly mentioned on behalf of completeness. In this case an electric field is induced by a current carrying coil in the plasma. Inductive methods are based on electromagnetic induction creating an electric vortex field with closed lines of force. The configuration acts as a transformer whereas the plasma represents one secondary winding. Power is transferred to plasma electrons by collisional dissipation and an ohmic heating process.[19,20] ICP is used for analytics in large devices such as ICP-MS, ICP-OES, ICP-TOF-MS. Of more significance for this review are capacitively coupled configurations. Essentially the discharge configuration consists of two electrodes separated by a certain distance; resembling a capacitor of an electric circuit leading to the term CCP. For capacitive methods, lines of force strike the electrodes and the resultant field is a potential field.

The capacitively coupled discharge can be classified by the frequency of the applied voltage and by the construction of the discharge cell (bare or dielectric covered electrodes); on the other hand the classification can be done by the physical processes in the gas discharge. According to the latter criterion, it may be assigned to one of two main groups, visualized in Fig. 1. Physically, they differ according to the discharge structure, practically the two modes can be switched by the discharge parameters such as gas pressure, applied frequency or discharge current. These two modes can be classified by the current density that can be above or below a certain critical current density j_c. For common systems the value of the critical current j_c as a function of the discharge frequency ω and the gas pressure p can be estimated as:

$$j_c = \frac{\varepsilon_0 B p \omega}{C + \ln(2p\mu E/\omega)},$$

where μ is the electron mobility, E the gap voltage and B, C constants characterizing the electrode material.[20] It can be derived from the equation that the critical current density j_c rises

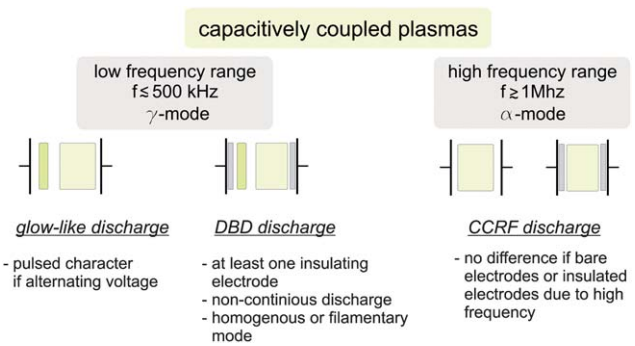

Fig. 1 Division of capacitively coupled plasmas into a low and high frequency range (γ- and α-modes respectively) considering bare and dielectric barrier electrodes.

with increasing frequency ω. For a discharge current density $j < j_c$ the discharge is carried out in the low current α-mode, since charge carrier multiplication happens mainly in the plasma volume (so-called α processes) and a bulk plasma is formed. For $j > j_c$ a high current density discharge takes place. This is referred to as γ discharge since the secondary electron emission from the electrode (γ process) starts being important. In this mode the discharge has a patterned structure, similar to a dc glow discharge. In both cases the electrodes can be either bare or covered with a dielectric layer referring to as insulated electrode discharge or DBD. It is important to note that the plasma in the α mode does not interact with the electrodes of the gas-discharge cell and therefore principally cannot be used for analyzing the electrode materials. It is important to notice that high and low current density does not refer to an absolute current density value. It refers to the current density related to the critical current density j_c given for a certain discharge system, frequency and pressure.

For a general overview, discharge classification in this review is carried out by frequency. The high frequency mode, described in this article, corresponds to an α-mode with a low current density with respect to the critical current j_c. The low frequency mode corresponds to a γ-mode with a high current density with respect to the critical current j_c.

High frequency range (α-mode)

CCP in the MHz regime are in the following denoted as capacitively coupled radio frequency (CCRF) discharges. A CCRF discharge is usually a weakly ionized, non-equilibrium plasma and its appearance resembles a homogeneous plasma. Especially for industrial applications, international conventions have specified a commonly used radio frequency of 13.56 MHz (and multiples) to avoid interference with radio broadcasting and communications.[20,21] The term radio frequency (rf) refers to alternating excitation voltages with frequencies larger than the ion plasma frequency $\omega_{p,i}$, but smaller than the electron plasma frequency $\omega_{p,e}$. Thus it can be assumed that due to their high mobility electrons respond instantaneously to the electric field and the ions remain fixed, forming a static positive space charge.[22]

The operation of CCRF plasmas is well understood: Due to their high mobility, electrons, which get in contact with the electrode, leave the bulk plasma at the electrode wall. To prevent electrons from leaving the plasma, a sheath layer develops adjacent to the electrodes. The sheath potential repels electrons and confines them to the bulk plasma. The ions remain static between the electrodes and the electrons oscillate within the positive space charge of the ions. In the sheath region, a depletion of electrons occurs leading to a violation of the quasi neutrality of the plasma.[19–21]

CCRF discharges can be driven with insulated electrodes as well, *i.e.* electrodes covered with a dielectric. Electrons of the plasma that incident the dielectric get attached at the surface, whereas the dielectric layer is charged producing an electric field repelling the further electrons. In the case of a CCRF with insulating electrodes the role of the sheath to repel electrons towards the bulk plasma is completed by the surface charges on the dielectric, *i.e.* nearly equivalent mechanisms take place. (Strictly speaking, a smaller sheath exists in this case as well, but the original function of the sheath layer is mainly taken over by the dielectric.) In the literature it is said in almost the same manner: A discharge with insulated electrodes does not differ from a discharge with bare electrodes, the dielectric layers have hardly impact onto the plasma.[21]

Low frequency range (γ-mode)

The main aspects we focus on in this review are plasmas at low frequencies up to kHz regime. The frequency is smaller than the electron and ion plasma frequency justifying a rough estimation that ions and electrons are able to follow the alternating field. At first, discharges with bare electrodes are considered. In the low frequency range they simply resemble a pulsed glow discharge and thus general information on glow discharges are provided.

Afterwards the dielectric barrier discharge (DBD) is introduced: the electrodes are covered with a dielectric, referred to as insulated electrodes.

A common glow discharge with bare electrodes ignited in the inter electrode gap and driven by a time independent dc voltage reveals the following mechanism. As the voltage is applied, free electrons are accelerated in the constant electric field performing ionization processes through collisions with neutral gas atoms. The avalanches of electrons and ions appear in the gas gap; the electron avalanches are accelerated towards the anode, the ion avalanches towards the cathode of the gas-discharge cell. The increase in the applied voltage results in exponential growth of the avalanche intensity. Above the breakdown voltage the avalanches are so intensive that the ion avalanches kick out electrons from the cathode material (γ process) and the self-sustained gas discharge is ignited.

The plasma has the patterned appearance of a glow discharge, including the bright negative glow and the cathode fall where the largest drop in electric field occurs. This prevents electrons from reaching the cathode and allows energetic ion impact on the cathode producing secondary electron emission to sustain the discharge. The positive column is a less intense region requiring only a weak electric field.

This breakdown mechanism of a self-sustained dc glow discharge is referred to as Townsend breakdown, it is expressed by the dependence of the breakdown voltage V from the product of pressure p times dimension d:

$$V = \frac{Bpd}{\ln(Apd) - \ln\left[\ln\left(1 + \gamma^{-1}\right)\right]}$$

Since the energy gain in electric field is essential for gas ionization, the 1st Townsend coefficient α represents ionization processes per length and electron (in the formula above included by a conventional empirical formula suggested by Townsend: $\alpha = Ap \exp(-Bp/E)$; with A, B empirically found in ref. 21). The 2nd Townsend coefficient γ represents secondary electron emission. The equation leads to the Paschen curve. It demonstrates the existence of a minimum breakdown voltage at a certain pd-value. This is essential for miniaturization of discharge devices, by decreasing the dimension to the μm regime, the optimal discharge pressure is approximately atmospheric pressure to take advantage of the minimum breakdown voltage. This

physical concept, called the scaling law, ensures a main advantage of analytical discharges: The dimensions are small and the operation pressure is around atmospheric pressure avoiding the use of bulky vacuum equipment.[21]

In contrast, a DBD requires the presence of one or more insulating layers and thus dc operation is precluded because of dielectric charging issues. DBDs are often operated under atmospheric pressure and are strongly non-equilibrium plasmas. Typically, square wave, sinusoidal wave or pulsed voltages between 500 Hz and 500 kHz[23] are used to drive a DBD by a displacement current which is determined by the dielectric constant and the thickness of the dielectric barrier.[17]

The homogeneity of the discharge may differ for different discharge conditions. The DBD discharge can reveal either a filamentary structure or a fairly homogeneous appearance. A filamentary discharge is characterized by individual micro-discharges or streamers which are stochastically distributed in space and time. In this case the breakdown mechanism is a streamer breakdown, an electron avalanche propagates through the gas gap creating manifold ions and the breakdown occurs without participation of the cathode.[24]

In the homogeneous mode a Townsend breakdown occurs and in contrast to the filamentary mode the discharge covers the entire electrode uniformly. The Townsend breakdown is driven by ionization (α) and secondary emission at cathode (γ) requiring slower ionization processes in the bulk gas than the streamer mode. Secondary emission at cathode or γ emission in the case of DBD is ensured by the existence of a dielectric and its memory effect which is later explained in detail. Homogeneous DBD plasmas are mainly observed in noble gases: due to Penning ionization processes (amongst others) bulk ionization is slowed down inhibiting streamer breakdowns and supporting the homogeneous noble gas dielectric barrier discharges. A detailed article of the mechanisms of homogeneous discharges was recently published by Massines *et al.*[24]

For a homogeneous DBD plasma the intensity distributions are similar to dc glow discharges; a region of bright intensity is formed at the cathode that can be identified with the negative glow region.[25,26] Unlike dc glow discharges, a DBD is a discontinuous plasma. It is driven by alternating voltages allowing theoretically one breakdown per half cycle. Thus, a homogeneous DBD can be identified with a glow discharge igniting only once every half cycle, whereas the dielectric acts as a barrier to extinguish the discharge after a short time of µs. Another difference is that the cathode position changes after each half-period. This ignition mechanism is explained in the following section, see Fig. 2. For simplicity, rectangular voltage is applied instead of a sinusoidal one.

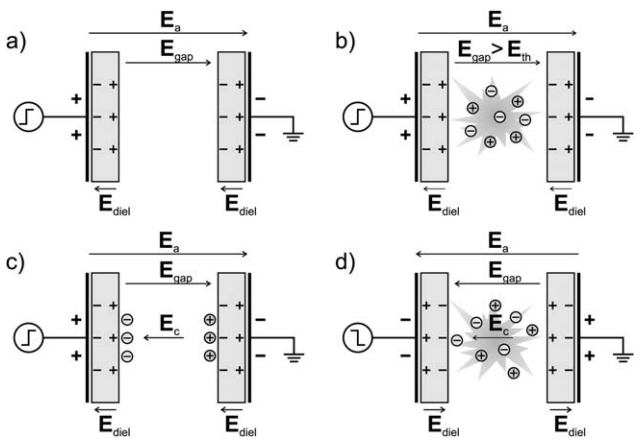

Fig. 2 Schematic explanation of the theoretical ignition mechanism of a dielectric barrier discharge of one half cycle.

Simultaneously with the high voltage pulse (E_a) an equivalent electric field establishes inside the capacitor. Due to displacement polarization the dielectric creates an opponent electric field reducing the electric field E_{gap} across the gas gap ($E_{gap} = E_a - 2E_{diel}$), see Fig. 2a. If E_{gap} reaches the threshold voltage for the given geometry and gas environment, a discharge ignites. Free charge carries are produced *via* collision ionization; this process is similar to a dc glow discharge (Fig. 2b). These free charges incident on the surface of the dielectric barriers and accumulate there. This reduces the electric field to $E_{gap} = E_a - 2E_{diel} - E_c$ leading to a termination of the discharge (different mobilities of charges are neglected in the scheme), Fig. 2c. In the following half cycle the polarity of the externally applied voltage is reversed. The memory effect of the surface charges that contributes to the secondary emission now supports the breakdown: $E_{gap} = E_a - 2E_{diel} + E_c$, see Fig. 2d. The dielectric layer on the one hand hinders the development of a continuous discharge and on the other hand it decreases the applied voltage required to reignite the plasma.

Example of a dielectric barrier discharge—a DB-MHCD setup

The following section shows an example of a DBD discharge operating in the γ-regime at low frequency. It is a miniaturized DBD plasma with the special electrode configuration of a hollow cathode, called dielectric barrier micro-hollow cathode discharge (DB-MHCD). The electrodes are covered with glass layers acting as a dielectric barrier. A sinusoidal high voltage of 1.5 kV and a rather low frequency of 1.5 kHz are applied to ignite a DBD plasma in a helium atmosphere. The arrangement of the setup is shown in Fig. 3a, and Fig. 3b reveals the measured voltage, current and emission curves. The sinusoidal current curve shifted by $\pi/2$ with respect to the applied voltage is the displacement current which is present during the entire cycle. The large current peaks reveal the short term plasma ignition, once during each positive half cycle and three times during each negative half cycle. The peaks are caused by conduction current of the charge carriers of the plasma (electrons and ions). They visualize the short term ignition of the plasma during each half cycle; the emitted light, shown by the grey line, is measured with a photomultiplier. This DBD plasma shows exemplarily the mechanism of DBD plasmas described above.

Analytical DBDs in the literature

1. Dielectric barrier discharges for elemental detection with optical spectrometry

In this section DBD for elemental detection is presented. The sample is directly introduced into the plasma and due to dissociation and excitation of the analyte optical spectrometry, mainly by emission and absorption, is carried out.

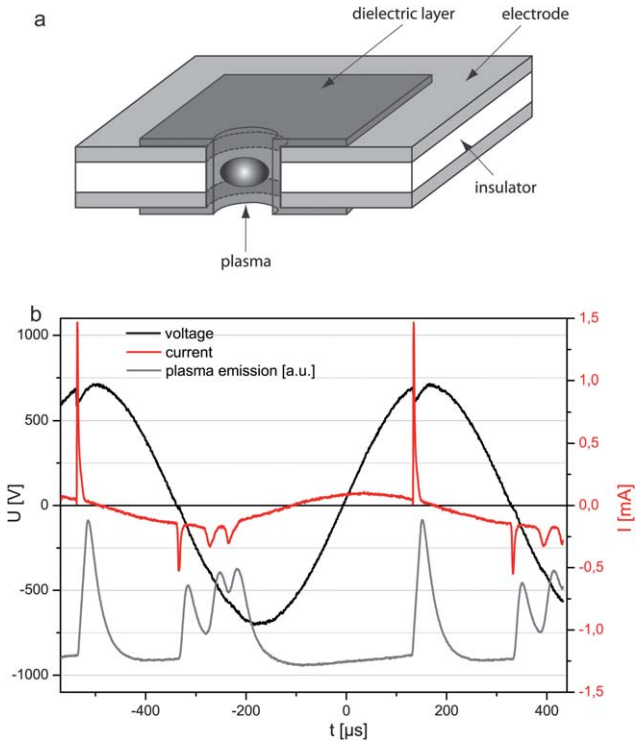

Fig. 3 Characterization of a miniaturized DB-MHCD plasma with electrode configuration of a hollow cathode. (a) Geometric configuration, and (b) current–voltage characteristic and plasma emission.

Planar DBD configuration coupled with DLAAS for halogenated hydrocarbons. One of the first DBD plasmas that is not used for ozone generation or plasma displays but for analytical applications was developed by Miclea *et al.* and is schematically shown in Fig. 4.[27] The discharge chamber consists of two glass plates covered with aluminium electrodes (50 mm length, 1 mm width) which are covered with a 20 mm thick glass-type dielectric layer. The glass spacers define a plasma channel of 1 × 1 × 50 mm^3. The discharge works at reduced pressures of 10–100 hPa in argon as well as helium with a gas flow of 10–1000 ml min^{-1} with applied rectangular voltages of 750 V_{pp} and 5–30 kHz. The DBD is ignited over the whole length of the electrodes. Plasma diagnostics revealed that the hot region of the plasma is constricted for a short time during each discharge cycle close to the temporary cathode. In this thin layer the electron density reaches a concentration of 10^{15} cm^{-3} and a gas temperature of about 1000 K, while the rest of the discharge remains cold.[25] Because the plasma ignition is pulsed the integral temperature in DBDs is rather low compared to direct discharges. The mean power consumption of the discharge is much smaller than 1 W. Measurements of halogenated hydrocarbons by diode laser atomic absorption spectrometry (DLAAS) in the dielectric barrier discharge were performed by absorption of excited atoms using a laser beam with a diameter of 1 mm along the discharge channel. The absorption signal was measured by a phase-sensitive detection using twice the modulation frequency of the DBD. The limits of detection of CCl_2F_2, $CClF_3$ or CHClF in the Ar DBD were 5 ppb v/v using the 837.824 nm Cl absorption line, which starts from a metastable level of Cl. In He the detection limits for CCl_2F_2 were 400 ppt v/v and 2 ppb v/v using the Cl 837.824 nm and the F 685.792 nm line, respectively. The authors proved that the absorption signals of Cl and F correspond to the stoichiometric ratios of these elements in the analyte molecules.[27] The capability of the small-sized dielectric barrier discharge as an element-selective diode laser atomic absorption detector for gas chromatography was further investigated. A chromatogram for various halogenated analyte molecules is shown in Fig. 5 (concentration of each species 300 ppb). Detection limits have been determined for halogenated and sulfured hydrocarbons in the pg s^{-1} range depending on the element measured. Furthermore, the effect of doping gas (oxygen) and make-up gas (argon, helium) on the chromatograms was studied.[28]

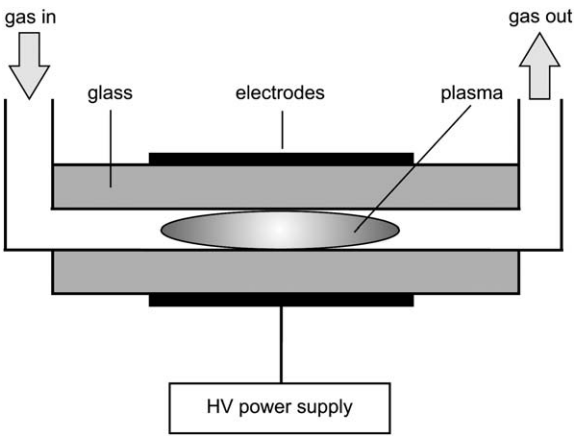

Fig. 4 Planar dielectric barrier discharge operated at 5–20 kHz for analysis of gaseous samples by DLAAS according to ref. 27.

Planar DBD configuration coupled with atomic absorption, fluorescence and emission spectrometry. Different optical techniques for the detection of elements with DBD were investigated by the group of X. R. Zhang in the last few years. Zhu *et al.* published a microplasma source based on a dielectric barrier

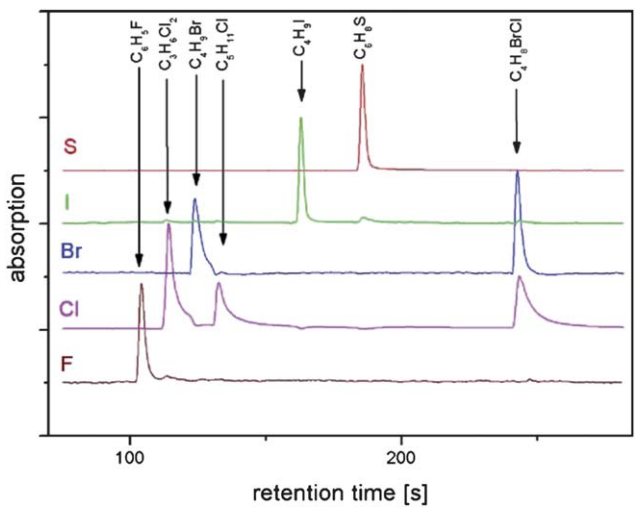

Fig. 5 Chromatograms for various halogenated molecules detected with element-sensitive DBD-DLAAS (concentration of each species 300 ppb), reproduced from ref. 28 with permission from Elsevier.

discharge as atomizer for AAS for arsenic speciation of hydrides.[29] The small plasma is generated under atmospheric pressure in Ar or He within a glass cell 3 × 8 × 70 mm^3 (Fig. 6) with applied voltages between 3.5 and 4.0 kV and a frequency of 20.3 kHz the power consumption of 5 W. Arsenic, antimony and tin analytes were investigated with the same systems with a LOD of 0.6 and 10.6 μg l^{-1}, respectively.[29] In a following publication with reduced sizes of the discharge channel, detection limits of this system for As(III), As(V), monomethylarsonic acid (MMA), and dimethylarsinic acid (DMA) obtained with hydride generation (HG)-DBD-AAS were found to 1.0, 11.8, 2.0, and 18.0 μg l^{-1}, respectively (Fig. 7). To assure the accuracy of the system, arsenic of reference materials was successfully verified.[30] In addition, the authors presented the determination of inorganic and total mercury by DBD-AAS.[31]

Furthermore a DBD-AFS setup was published by the same authors[32,33] for atomic fluorescence measurements. The DBD was ignited in a cylindrical configuration with a slightly larger inner diameter of 4 mm. An argon discharge was characterized by a power of 13.5 W, with excitation voltages of 4.3–7.0 kV at 20 kHz. The detection limit of As(III) using hydride generation with the proposed DBD–AFS was 0.04 μg l^{-1}. Further, analytical results obtained for reference values agreed well with the certified values. For Sb and Pb the detection limits were in the same range 0.11 μg l^{-1} and 0.27 μg l^{-1}, respectively.

In a following publication Zhu *et al.*[34] presented an approach for the determination of mercury by atomic emission spectroscopy (DBD-AES). In contrast to the latter setups, the plasma is ignited in reduced dimensions (glass cell 0.6 × 1 × 10 mm^3) and requires less than 1 W power.

Hg vapour for detection is separated from the sample solution by a commercial ICP concentric pneumatic nebulizer and transported by the carrier gas to the DBD atomizer cell. The low temperature of the DBD did not cause any thermal stress. The authors show emission spectra revealing the presence of Hg clearly. They further noted that introduction of water vapor causes lower continuum background and molecular emission which increases the signal to noise ratio. This indicates that the DBD can be operated advantageously without the removal of residual water vapor leading to simplification of sample introduction. Detection limits of this configuration were found to be 14 pg ml^{-1} Hg (He-DBD) and 43 pg ml^{-1} (Ar-DBD), respectively.

Dielectric barrier discharges for emission and fluorescence spectroscopy were presented by the group of J. Wang. For the analysis of mercury vapor an atmospheric pressure dielectric barrier discharge is used as radiation source for optical emission spectroscopy (OES) demonstrated by Yu *et al.*[35] Fig. 8 shows a typical setup: the discharge is ignited inside a planar electrode configuration. The discharge covers a volume of 50 × 5 × 1 mm^3 with two quartz plates (a thickness of 1.2 mm) serving as a dielectric barrier and the planar electrodes are made of aluminium. The discharge is ignited and maintained in argon by an ac neon power supply with a frequency of 35 kHz and a homogeneous plasma is observed at 1.2–1.8 kV. Sample introduction is achieved with mercury cold vapor generation by a micro-sequential injection unit. The optical emission of mercury is recorded at 253 nm in the emission spectra and calibration measurements lead to a detection limit of 0.2 μg l^{-1} for Hg, analytical results are depicted in Fig. 9. The publication shows that the detection limits of the present DBD-OES system are comparable with other OES measurements of mercury usually performed direct plasma discharges. Furthermore, mercury in certified reference materials is examined, showing a reasonable agreement between the certified and obtained values.

In a following publication Puanngam *et al.* developed an automated atmospheric mercury analyzer based on a gold-on tungsten coiled filament preconcentrator, DBD atomic emission and a radiation detector.[36] The preconcentration is needed for purposes of sensitivity and further eliminates the ambient humidity which decreases the emission signal. Mercury from the atmosphere is preconcentrated for 2 min and flushed with the argon flow into the DBD plasma. Detection limits are estimated to 0.12 ng l^{-1} of mercury, the linear range is extended to

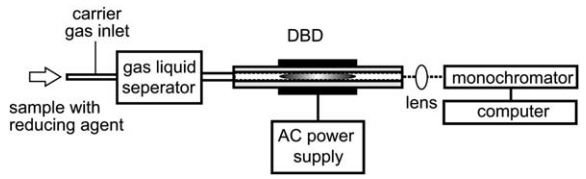

Fig. 6 Schematic setup of planar DBD for elemental detection with AAS, AFS and AES according to ref. 34. For sake of the overview, the radiation source for AAS, AFS is excluded.

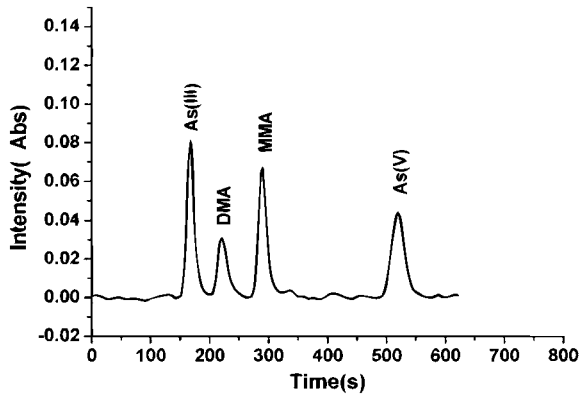

Fig. 7 Separation of arsenic species (As(III), As(V), MMA, and DMA) by HPLC with the HG-DBD-AAS detection (sample mixture of As-(III) (100 μg l^{-1}), As(V) (100 μg l^{-1}), MMA (100 μg l^{-1}), and DMA (100 μg l^{-1}); sample volume 100 μl), reproduced from ref. 30 with permission from ACS Publications.

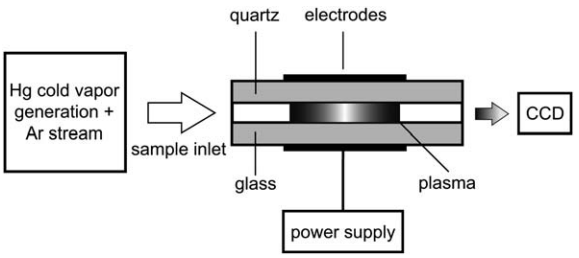

Fig. 8 Schematic of the miniature DBD-OES system for analysis of mercury vapor according to ref. 35.

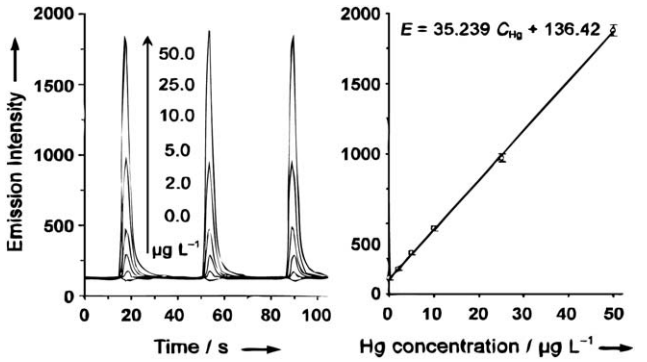

Fig. 9 The recorded peak shapes and the calibration graph for 0.0–50.0 µg l^{-1} Hg^{2+} (500 ml of sample solution in HCl (1.0%, v/v) and 400 ml of $SnCl_2$ solution (3.0%, m/v); 1.50 kV), reproduced from ref. 35 with permission from Wiley.

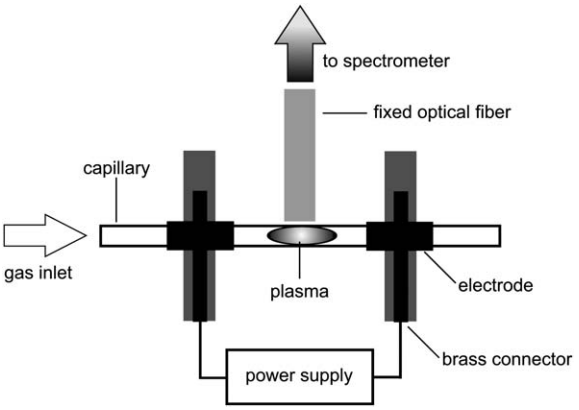

Fig. 10 Microplasma in a fused silica capillary for OES of gases presented in ref. 39.

6.6 ng l^{-1}. To demonstrate the DBD-OES detector for atmospheric mercury, the authors carried out field application measuring mercury concentrations at a fluorescent lamp recycling plants verifying the functionality.

Furthermore Yu *et al.* developed a miniature lab-on-valve atomic fluorescence spectrometer (AFS) with an integrated DBD atomizer for the analysis of arsenic.[37] The hydride generation technique is employed for pretreatment of the arsenic solution and *via* gas–liquid separation isolated hydrates are flushed by an argon flow into the DBD atomization chamber dissociating the sample into free arsenic atoms. Atoms are transported to a detection chamber to be excited by incident light from a hollow cathode lamp and the fluorescence is monitored. The DBD configuration is planar with the size of 4 × 3 × 30 mm^3 and is driven by an ac neon power supply. Homogeneous argon DBD plasmas are obtained by applying output voltages between 1080 and 1590 V. Further increase in voltage improves atomization efficiency and fluorescence signal but degrades the stability and the homogeneity of the plasma. Advantageous for the DBD atomizer is the cold nature of the discharge. Standard atomizers use temperatures of a few hundred degrees releasing large amounts of heat which makes the integration of the light source, atomizer and detector into a compact space and the miniaturization of the detector system impossible. Analytical measurements of the arsenic AFS signal revealed a detection limit of 0.03 µg l^{-1}, similar to those obtained by commercial AFS instruments.

Capillary DBD coupled with emission spectrometry. An atmospheric pressure microplasma in a fused silica capillary was designed by the group of P. C. Hauser for element analysis *via* atomic emission spectrometry of organic and inorganic gases separated *via* gas chromatography.[38–41] The microplasma works at 20 kV and 20 kHz by capacitive coupling of the energy into the capillary. The setup shown in Fig. 10 consists of a capillary with two cylindrical electrodes placed at a distance of 1 cm around the circumference of the capillary (250 µm i.d., 350 µm o.d.). To prevent deterioration of the electrodes and contamination of the plasma with electrode metal the electrodes have no direct contact with the plasma. Although the authors identified the discharge as capacitively coupled, it can be considered as a dielectric barrier discharge (due to the low frequency applied) where the charges accumulated on the glass play a relevant role in switching off the discharge.

The microplasma can be supported at a flow rate range corresponding to most common capillary chromatographic methods at atmospheric pressure, namely 5 ml min^{-1} and the applied power is 8 W.

The microplasma was implemented as an on-column optical emission detector. The optical fiber was coupled directly above the capillary directing the emitted light to a spectrometer. The plasma was self-igniting after the passage of the solvent through the capillary.

The detection of organic compounds by monitoring the emission signals of C, Br, Cl, F, I, P, Se, and S separated in a helium carrier was possible. The authors reported the determination of environmentally relevant halogenated volatile organic compounds and pesticides. Halogens (F, Cl, Br, I) and sulfur were measured by monitoring the emission lines at 685.60, 837.59, 827.24, 804.37, and 921.28 nm, respectively, see Fig. 11. The obtained detection limits are F 20 pg s^{-1}, Br 0.3 pg s^{-1}, Cl 0.1 pg s^{-1}, I 158 pg s^{-1}, and S 6.6 pg s^{-1}.[38]

In a further publication Guchardi *et al.* demonstrated the detection of inorganic compounds with carbon containing species (CH_4, CO, CO_2) from the emission band of CN at 385 nm and with H_2, O_2, SO_2, NO_2 gases by emission of atomic H (656 nm), O (777 nm) and S (923 nm). Detection limits are in the range of 9.0–0.2 ng per injection, except H_2 and NO_2 show extremely high limits of 14 and 87 ng, respectively. It has to be noted that the concentration detection limits for gaseous species of approximately 0.5% vol in the gas phase are not adequate for trace determinations in environmental monitoring but should be suitable for industrial application.[41]

DBD-liquid electrode setup for aqueous analysis. A novel approach for the analysis of liquid samples is the electrolyte as cathode discharge (ELCAD), developed by Jenkins and Manz,[42] which is an effective method for liquid sample introduction. Later on, an ELCAD configuration to establish a glow discharge for analysis of aqueous samples was introduced by the group of G. M. Hieftje.[43,44] Although these articles did not pursue the DBD principle, subsequent publications combine DBD and

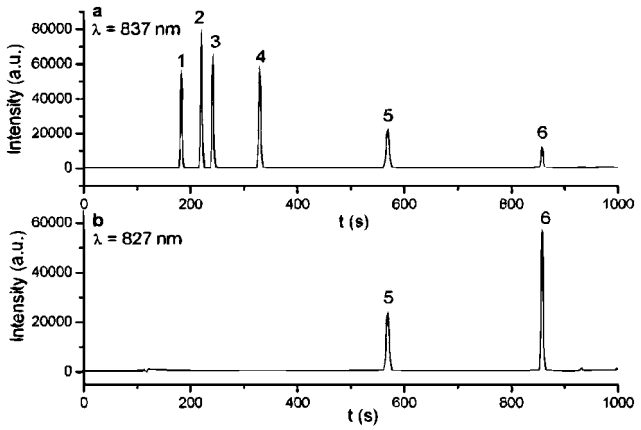

Fig. 11 Chromatograms for a mixture of halogenated organic compounds (2000 mg ml^{-1} each). (a) Emission from Cl; (b), emission from Br (1) 1,1-dichloroethylene, (2) methylene chloride, (3) *trans*-1,2-dichloroethylene, (4) *cis*-1,2-dichloroethylene, (5) bromodichloromethane, (6) dibromochloromethane, reproduced from ref. 38 with permission from The Royal Society of Chemistry.

ELCAD. For the analysis of metal containing liquids by optical emission spectrometry a micro-tube-based system is presented by Tombrink *et al.*[45] It is based on a miniaturized dielectric barrier discharge driven at atmospheric pressure. Emission lines of various elements are observed, an example for Sr is depicted in Fig. 12. The system is developed for quantitative measurements and the limits of detection are determined. Because of very low flow rates of just µl min^{-1} the approach requires extremely low sample volumes. This analysis system is supposed to be hyphenated with micro-separation devices, for example µHPLC and integration on a µChip seems to be possible in the future.

The setup is schematically shown in Fig. 13, consisting of a 100 mm long fused silica polyimide-covered capillary (250 µm i.d., 350 µm o.d.) covered with copper layers serving as electrode. The end of the capillary stays open to ambient air and a tungsten wire is connected over a 680 kΩ—resistance to ground. The advantage of this system is that the electrodes will not be sputtered or oxidized. Hence the electrodes are stable for a long time and the measurement is not falsified. The sample solution is

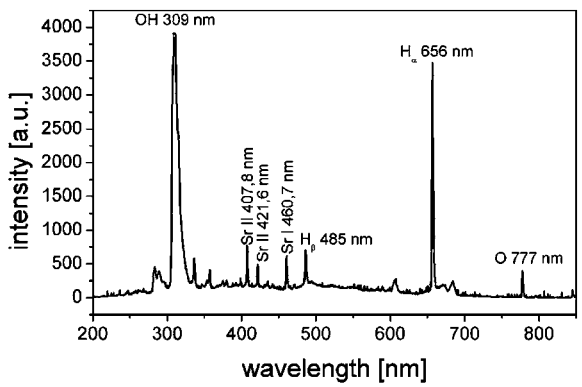

Fig. 12 Emission spectra of liquid electrode DBD setup, Sr analyte concentration of 880 µg l^{-1}, reproduced from ref. 45 with permission from Springer.

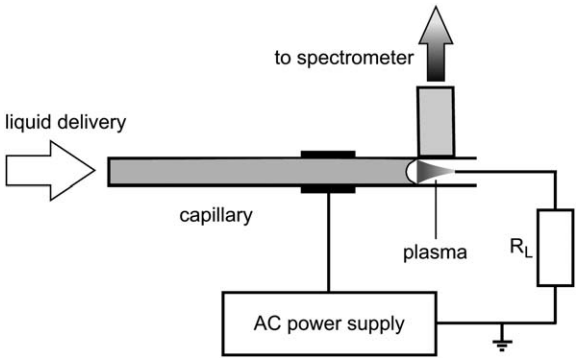

Fig. 13 Schematic setup of the miniaturized DBD with liquid electrode according to ref. 45.

acidified with HNO_3 to a concentration of 1 mol l^{-1} and for electrolyte delivery the capillary is connected to a syringe pump system with a flow rate of 1 µl min^{-1}. For initiation of the DBD with liquid electrode a custom build generator with a positive voltage peak output signal of 2.3 kV at 40 kHz is applied.[46]

For sodium a calibration was carried out with a detection limit of 64 µg l^{-1}. In this way it is possible to accomplish a measurement in 1 s. Calibration curves were prepared for Sr, Pb, and Hg and limits of detection were 18, 40, and 42 mg l^{-1}, respectively.

A microplasma generation in a sealed microfluidic glass chip using a water electrode was demonstrated by Jo *et al.* for the application of the miniaturized chemical detection system, especially for water contaminants.[47] The microstructured glass substrate is employed to isolate the water sample from the metal electrode. An ac voltage (50 kHz, 1 kV) applied to the bottom metal electrode is transmitted to the water chamber capacitively allowing a voltage drop along the microchannel. The authors analyzed the behavior of a micro-bubble by using 1% NaCl by taking images with a high-speed-camera to show that it takes 1 s from the ignition to a stable state discharge. The detection of Pb using a dilution series of a standard lead concentration of 100 ppm in 0.1 M HNO_3 is determined by measuring and calibrating the emission line at 406 nm. The LOD is located at 10 ppm, but could be lowered by improving optical arrangement according to the authors.

2. Dielectric barrier discharges as ionization source for analytical application

This section summarizes articles on dielectric barrier discharges serving as an ambient ionization tool for molecular speciation. Fundamental mechanisms are radical formation and in significantly larger numbers soft ionization processes. The detection of molecules is performed by mass spectrometry, ion mobility spectroscopy and chemiluminescence.

This section includes as well DBDs that are employed to enable or facilitate chemical reactions. Due to the fact that molecular detection is carried out with mass spectrometry, these applications are included in this section, although the DBD is not necessarily used as ionization source.

DBDI for MS analysis. The group of X. R. Zhang introduced a new ion source based on dielectric barrier discharge as

alternative ionization source for ambient mass spectrometry in 2007.[48] The dielectric barrier discharge ionization (DBDI) consists of a hollow stainless steel needle (20 mm long, 0.2 mm i.d.) used as the discharge electrode. A copper sheet (25 × 75 mm) serves as the counter electrode. A glass slide is placed on top of the copper sheet acting as both dielectric barrier and sample plate, see Fig. 14. By applying an alternating voltage (20.3 kHz, 3.5–4.5 kV) and a supporting He gas flow of 50 ml min^{-1}, a discharge was formed between the tip of the discharge electrode and the surface of the glass slide. The plasma and its energetic electrons are able to desorb and ionize analytes deposited on the glass slide and the ions are analyzed *via* mass spectrometry (MS). Fig. 15 shows exemplarily mass spectra of amino acids (L-valine M_r 117, L-proline M_r 115, L-serine M_r 105, and L-alanine M_r 89). The base peaks can be identified with protonated molecular ions $[M + H]^+$ that are generated in the discharge process accompanied by characteristic fragment ions. In a subsequent publication Na *et al.* demonstrated the direct detection of explosives TNT, RDX, PETN that are deposited on solid surfaces with DBDI source.[49] Detection limits are in the range of 10 pg to 1 ng for the above mentioned explosives allowing the detection on various matrices like paper, cloth, chemical fiber, glass, paints, and soil.

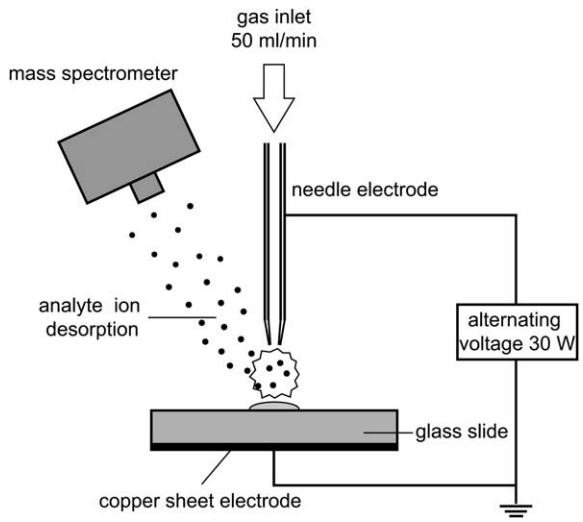

Fig. 14 Schematic setup of the DBDI source according to ref. 48.

LTP for MS analysis. A different plasma configuration was introduced by the group of R. G. Cooks in 2008.[50] The configuration is denoted as low temperature plasma (LTP) due to the moderate plasma temperature. The LTP probe consists of a glass tube (6.35 mm o.d., 3.75 mm i.d.) with an axially centered electrode made out of stainless steel (diameter 1.57 mm) serving as the grounded electrode, see Fig. 16. Copper tape wrapped around the glass tube serves as the outer electrode connected to the HV source (2.5–5 kV, 2–5 kHz). The discharge ignites in He, Ar, N_2 and air with flow rates of approximately 0.4 l min^{-1}. The low temperature plasma exits the glass tube and interacts with the sample directly where it desorbs and ionizes surface molecules in the ambient environment. The main ions generated are protonated molecules $[M + H]^+$ with minimal fragmentation. In contrast to the above introduced DBDI source, this plasma configuration allows direct interaction of the plasma with the sample. The plasma can be directed to any kind of object, they may be fixed, small, large, *etc.* Due to the low temperature, the LTP can further be used for desorption on human skin.

Harper *et al.* present various application fields for the LTP ambient ionization technique:[50] Explosive analysis leading to a LOD of TNT of 5 pg; the analysis of cocaine on human skin (see Fig. 17) and the direct ionization of chemicals from bulk aqueous solution have been demonstrated as well with detection limits of 1 ppb.

In a following paper Zhang *et al.* reported a LOD of TNT of 500 fg and effects of the discharge gas and power were analyzed. Further the direct detection of explosives on both conductive and non-conductive surfaces was shown making this LTP probe a versatile ionization technique for MS.[51] The rapid screening of pharmaceuticals was also shown by the same group successfully, allowing the detection of 600 samples within 1 h.[52]

Ma *et al.*[53] demonstrated the real-time monitoring of organic chemical reactions by mass spectrometry utilizing the LTP probe by directing the plasma to the surface of the reaction system. The monitored reactants and products include polar and non-polar organic compounds. This proved that the ionization process with a dielectric barrier plasma, the LTP probe, is a simple approach

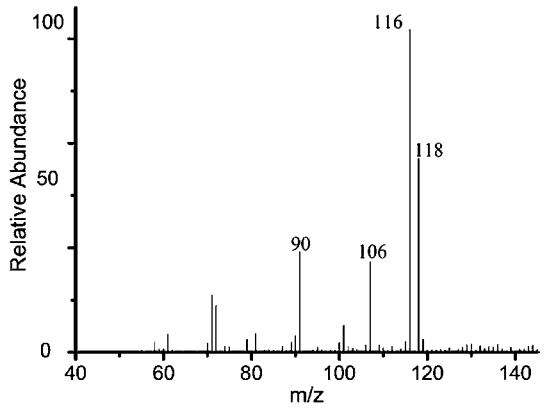

Fig. 15 Characteristic mass spectra for amino acids, reproduced from ref. 48 with permission from Elsevier.

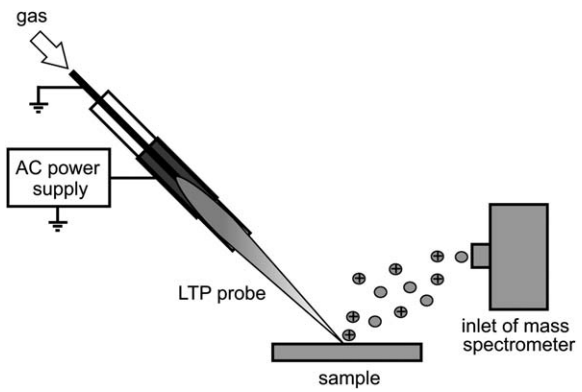

Fig. 16 Schematic of the configuration of the LTP probe for ambient ionization MS according to ref. 50.

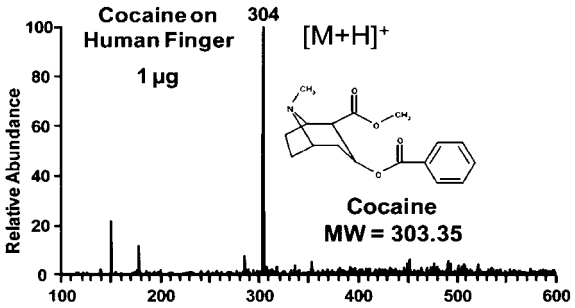

Fig. 17 Analysis of cocaine on human skin using the LTP probe reproduced from ref. 50 with permission from ACS Publications.

for reaction monitoring with least requirements for experimental devices and procedures.[53]

Almasian *et al.* developed a graphite LTP probe with a dual mode fragmentation selectable by an electrical switch for ambient MS.[54] The setup is similar to the previously described ones whereas the axially centered electrode connected to the ac voltage is made out of graphite. It is operating in two modes, in mode A a copper electrode underneath the glass slide serves as second electrode and in mode B a copper foil around the capillary acts as second electrode alternatively. In contrast to the previous application of the LTP probe, volatile organic compounds are introduced with a supporting Ar flow directly into the capillary. Both modes show different fragmentation patterns, which might be applicable in identification studies according to the authors.[54]

Recently, the same group demonstrated the application of LTP to elemental analysis of solids. Depth profiling experiments of nanometre coating by LTP and elemental analysis with ICP-MS were proven in ref. 55. The setup is slightly different from the previously described LTP probes, whereas in this publication both electrodes are placed around the capillary. The sample material is ablated by the LTP probe (2.5 kV, 10 kHz, 30 W), converted into an aerosol and then analyzed by ICP-MS. Ablated holes have a diameter less than 10 µm and a lateral resolution of approximately 200 µm has been achieved. Examples of depth profiling of multilayer samples (100 nm Al, 250 nm SiO_2, 100 nm Au, 50 nm Cr) have been performed and the different layers are properly resolved. However, analysis of light elements was not proven.

Publications on the application of LTP probe described above carried out by the groups of R. G. Cooks and A. Molina-Díaz: Huang *et al.* presented high throughput analysis of melamine in complex mixtures by using the LTP ambient ionization combined with tandem mass spectrometry (MS/MS).[56] Melamine in milk powders, whole milk and other products were detected and quantified at levels down to the ppb with an analysis time of few tens of seconds. The same authors described the combination of LTP with a handheld mass spectrometer.[57,58] Melamine detection limits were in the range of 0.03–0.5 µg l^{-1} depending on the matrices. The combination of LTP and the portable mass spectrometer Mini 10.5 is shown to be a robust method with high throughput satisfying requirements for realistic *in situ* analysis.

Garcìa-Reyes *et al.* demonstrated the direct analysis of olive oil by LTP ambient ionization mass spectrometry to detect free fatty acids, selected bioactive phenolic compounds and volatiles.[59] Furthermore Jackson *et al.* showed the analysis of drugs of abuse by LTP.[60] In general it can be seen that various application fields of the well developed LTP probe based on the dielectric barrier principle can be expanded from analysis of gases and liquids to analysis of solids by ablation.

The influence on a DBD to chemical reactions is further demonstrated in a publication by Y. Xia *et al.*[61] For peptide and protein analysis, nanoelectrospray (nanoESI) soft ionization is a favourable method. The authors report peptide fragmentation after pretreatment of the nanoESI emitters with a helium low-temperature plasma with a dielectric barrier principle. The plasma is turned on for 2 min enclosing the emitter. After the plasma is turned off, a high voltage is applied to the nanoESI containing the peptide solution and mass spectra are recorded. Note that the nanoESI is not operating during discharge ignition. With emitter pretreatment, unique fragmentation patterns of peptides are observed. The types of fragments include a-, b-, and y-type ions. This feature of DBD application is attractive for structural characterization of peptides. It is suggested that the DBD plasma releases electrolytes from the glass emitter so that they can be taken up into the spray solution causing a high local electrolyte concentration. The fragmentation is supposed to be related to ion formation under these special ESI conditions.[61] In this publication, the DBD is solely used for pretreatment and not as ionization source. It shows that ESI, a commonly accepted soft ionization technique, can act with DBD pretreatment as a hard ionization technique as well.

Furthermore, DBDs are used to facilitate gas phase chemical reactions, such as the Birch reduction by the groups of X. R. Zhang and R.G. Cooks.[62] The dehydrogenation of benzene and other arenes takes place in a low temperature plasma (LTP). Therefore a planar He DBD is ignited between glass slides inside a rectangular channel ($8 \times 65 \times 1$ mm^3). Copper sheets acting as electrodes are attached on both sides of the glass slides and the discharge is driven by an alternating voltage of 3 kV_{pp} and 20.3 kHz. Helium and the benzene sample are fed into the discharge and the resulting ionic species are introduced into a mass spectrometer. Mass spectra of benzene and other arenes indicating Birch reduction are shown in Fig. 18. The major signal has a mass of 2 Da above that of reactant $[M + 2H]^+$ caused by dihydrogenation. For benzene (C_6H_6), the reduction stops after the addition of two hydrogen atoms forming cyclohexadiene products (C_6H_8). Neither molecular radical ions M^+ nor protonated molecules $[M + H]^+$, which are normally detected using DBD ambient ionization techniques, are observed. The authors suggest that the benzene occurs at the discharge surface and is initiated by the capture of low-energy electrons followed by protonation of acidic hydrogen atoms from surface hydroxy groups of the glass dielectric barrier.[62]

Capillary DBD-plasma jet for IMS/MS analysis. A miniaturized excitation source for soft ionization of molecules based on a dielectric barrier discharge was first reported by the group of J. Franzke demonstrating measurements of gaseous compounds with ion mobility spectrometry in 2007[63,64] and with mass spectrometry in 2009.[65] An atmospheric plasma is established in a fused silica capillary (500 µm i.d., 1200 µm o.d.) using He buffer gas and electrodes around the capillary with a separation

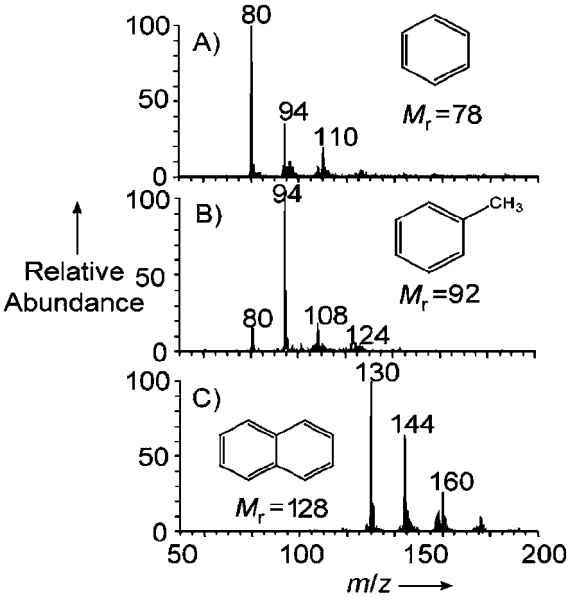

Fig. 18 LTP mass spectra indicating dehydrogenation of (A) benzene, (B) toluene, and (C) naphthalene, reproduced from ref. 62 with permission from Wiley.

distance of 12 mm, see Fig. 19. With applied peak voltages of 5–6 kV, frequencies between 20 and 30 kHz and a gas flow rate of 250 ml min^{-1} a plasma jet emerges into the ambient air outside the capillary. This part of the plasma is used as soft ionization source. In ref. 64 experiments were carried out by comparing plasma ion mobility spectrometry (IMS) and β-radiation IMS demonstrating that plasma IMS is found to be a stable and efficient ionization source. It is characterized by higher sensitivity and selectivity than β-radiation IMS. This is exemplarily shown with a detection limit of 2-nonanone of 10 ppt v/v with plasma jet ionization (β-radiation IMS 1000 ppt v/v) presenting the great potential of DBD ionization systems.

Furthermore, the application of the capillary DBD jet for liquid chromatography/mass spectrometry is demonstrated.[65] The plasma jet is compared to conventional electrospray ionization (ESI), atmospheric pressure chemical ionization (APCI), and atmospheric pressure photoionization (APPI) in the positive ionization mode. A heterogeneous compound library was investigated that covered polar compounds such as amino acids, water-soluble vitamins, and nonpolar compounds like polycyclic

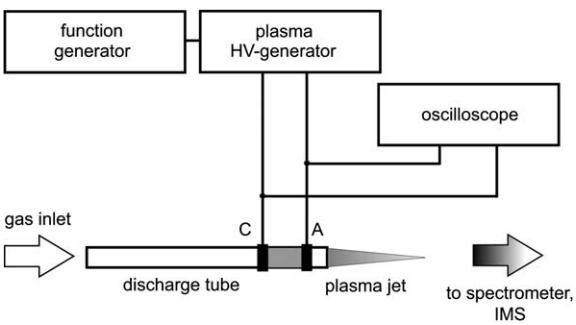

Fig. 19 Schematic configuration of the DBD plasma jet ionization source for IMS/MS according to ref. 63.

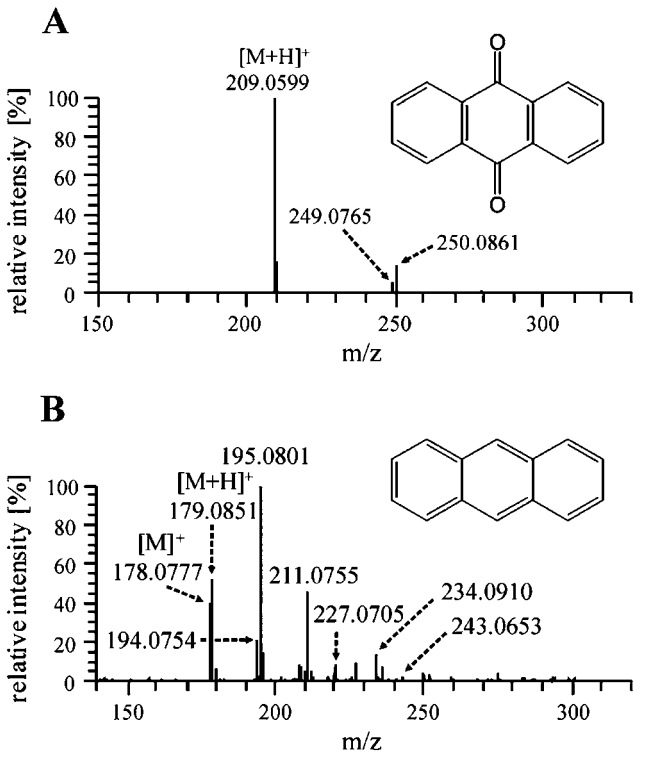

Fig. 20 Plasma jet DBDI-MS spectra of selected polycyclic aromatic model compounds 9,10-anthraquinone (A) and anthracene (B), reproduced from ref. 65 with permission from ACS Publications.

aromatic hydrocarbons and functionalized hydrocarbons. It turned out that DBDI can be regarded as a soft ionization technique characterized by only minor fragmentation similar to APCI, whereas mainly protonated molecules are detected. In general, compounds covering a wider range of polarities can be ionized by DBDI than by ESI; the ionization of a polar and non-polar compound is depicted in Fig. 20 exemplarily. Furthermore, limits of detection compared to APCI are in most cases equal or even better.

To provide an explanation of the ionization mechanism spectroscopic characterization of the plasma jet was carried out in following publications.[63,66] It was shown that nitrogen plays an important role for soft ionization: The present capillary DBD jet produces primary N_2^+ ions not only by electron impact but mainly by Penning ionization due to high helium metastables. N_2^+ ions generate protonated water clusters, so-called reactant ions, which in turn protonate analyte molecules. It is shown that for plasma jet IMS soft ionization helium as buffer gas is essential.

Dielectric barrier electrospray as an alternative ionization technique for MS. Besides dielectric barrier plasma discharges that are inherently linked to characteristic optical emission, the group of J. Franzke introduced a new discharge type of an electrospray driven by dielectric polarization as alternative ionization source (DB-ESI).[67–69]

Commercial electrosprays with platinum coated nanospray emitters reveal erosion of the electrode after electrospray procedure affecting the electrolyte solution and leading to

unstable electrosprays. Unlike this, for the DB-ESI approach the metal electrode is separated from the liquid analyte through a non-conductive layer and the electric field for the electrospray is generated by dielectric polarization across the insulating layer.[67] Stark *et al.* presented a setup for the electrospray interface shown in Fig. 21 composed of a fused silica capillary (360 μm o.d., 50 μm i.d) coated with a thin copper film as the contact electrode (few 100 nm thickness about 10 mm long) and a nanospray emitter (360 μm o.d., 20 μm i.d., 10 μm orifice not coated). Like dielectric barrier discharges, the DB-ESI is a discontinuous process requiring an alternating potential. The electrospray is driven by a square wave HV voltage of 5 kV and frequencies of a few Hz. With flow rates of 0.1 μl min^{-1} a taylor cone is initiated and an electrospray established.[68]

This technique allows mass spectrometric measurements in the positive as well as in the negative mode. Due to low currents, undesired discharges are avoided. This ionization method provides ions from liquids at atmospheric pressure for MS. Mass spectrometric measurements carried out with an ion-trap mass spectrometer of reserpine in positive and negative ion mode are shown verifying the applicability of the novel DB-electrospray ionization method. In a following publication, Stark *et al.* proved with the analysis of solution of 10 μM lysine that mass spectra obtained with DB-ESI are identical to conventional ESI which is indicated by the same isotopic ratio. An increase in the signal intensity of 80% was measured with DB-ESI in contrast to conventional ESI[69] which is demonstrated in Fig. 22. Besides widespread DBD plasmas, this DB electrospray discharge presents a new application field of dielectric barrier discharges in analytical chemistry.

DBD coupled with chemiluminescence detector. With the dielectric barrier discharge-induced chemiluminescence (DBD-CL) detector the group of X. Hou introduced a new application of DBD in analytical atomic spectrometry.[70] Chemiluminescence (CL) is the emission light by chemical reaction. Radicals (reactive oxygen species) oxidize a CL reagent to emit intense light. In the presented work a DBD plasma is used for radical generation. It is assumed that on the one hand the high density of energetic electrons of the DBD (10^{15} cm^3) is responsible for the dissociation ability of the DBD and furthermore the UV irradiation emitted by the DBD is well known as an efficient source to dissociate compounds and generate radicals.

The DBD-CL setup consists of two major parts, a DBD device and a commercial luminescence analyzer, see Fig. 23. The atmospheric pressure DBD plasma is used to split and excite organic compounds. The discharge is established within a glass tube (3.0 mm i.d. × 4.0 mm o.d. × 20 mm long) serving as a dielectric barrier with a thickness of 1 mm. The electrodes are made of metal wire, one is inserted in the glass tube and the second is wrapped around the outer side of the dielectric barrier. A compact ac ozone generation power with 4 kV and 20 kHz is applied to the discharge with an input power of 5 W and power adjustment through a transformer. The discharge is ignited with nitrogen gas with a flow rate of 300 ml min^{-1}. Subsequently the substances from the DBD and the CL reagent are mixed and flushed through the detection coil for CL detection of the BPCL analyzer.

Regarding emission intensities, signal to noise ratios and availability the most suitable electrode material is copper and the most effective discharge gas is N_2. Twelve different volatile organic compounds are tested, including methanol, ethanol, propanol, formaldehyde, dichloromethane, tetrahydrofuran, carbon bisulfide and ethyl ether. CL emission was observed, although different intensities and peak shapes occurs. For example chlorinated hydrocarbons produce strong CL emission, while carbon bisulfide is much weaker.

The CL signal is proportional to the analyte concentration and is affected by DBD parameters. Calibration measurements are carried out revealing a limit of detection is below 0.1 μg per injection for analytes like ethanol, propanol, formaldehyde and acetaldehyde.

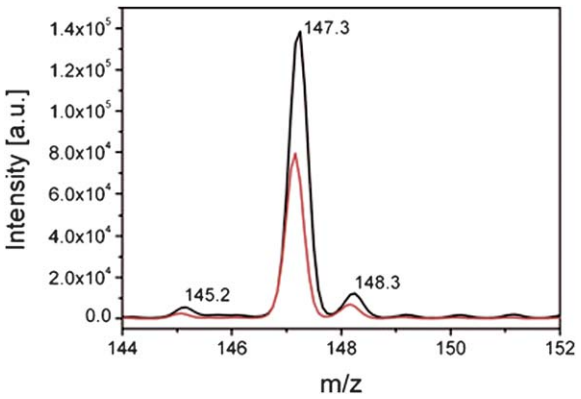

Fig. 22 Mass spectra of lysine employing both DB-ESI (black) and conventional ESI (red); flow 0.3 μl min^{-1}; 10 μmol l^{-1} lysine in 0.1% formic acid; 20 μm i.d. emitters; emitter-to-MS distance, 3 mm; $U_{DB\text{-}ESI}$ 5.5 kV; $U_{convent\ ESI}$ 1.5 kV, reproduced from ref. 69 with permission from Springer.

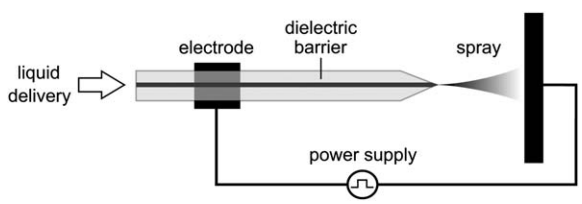

Fig. 21 Experimental setup for dielectric barrier electrospray ionization (DB-ESI) for mass spectrometric detection according to ref. 68.

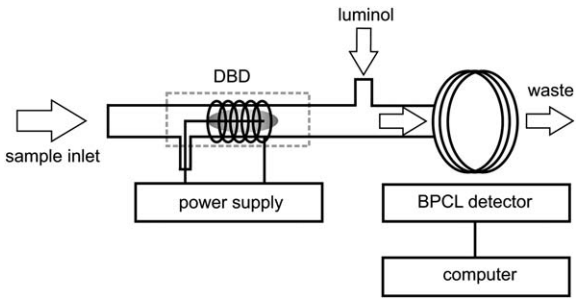

Fig. 23 DBD-CL setup consisting of two major parts, a DBD device and a commercial luminescence analyzer, according to ref. 70.

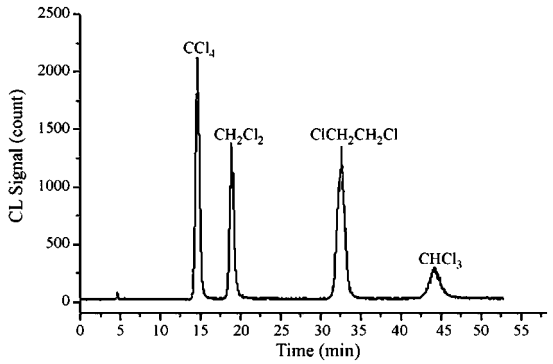

Fig. 24 Chromatogram showing the separation of VCHCs by GC with the DBD-CL detector. The injected quantities of the mixtures were 3 nmol for CCl_4, 7 nmol for CH_2Cl_2, 7 nmol for $ClCH_2CH_2Cl$, and 6 nmol for $CHCl_3$, reproduced from ref. 71 with permission from Elsevier.

A subsequent publication of the same group demonstrates the application of DBD-CL detector for volatile chlorinated hydrocarbons (VCHCs) separated by gas chromatography.[71] A characteristic chromatogram is shown in Fig. 24. Calculated limits of detection for VCHC are 2–4 pmol for dichloromethane, chloroform, *etc.* revealing high sensitivity of the detector. The publication further presents a possible mechanism for dissociation of the VCHC in the DBD to provide an understanding of the predominant mechanism.

Conclusion

This article shows that the concept of dielectric barrier discharges for analytical chemistry is well developed and hopefully contributes to the understanding of DBD whereas the fundamental mechanism of the DBD is explained. Up to now DBDs are very versatile covering a wide range of detector systems and ionization sources. Advantages of this discharge type are less analyte contamination by erosion of the isolated electrodes and a longer life time compared to other miniaturized discharges due to a lower integral temperature. Furthermore the DBD plasma can offer a rather non-destructive character making it applicable for not only dissociation techniques. This is visible in the two fields of application. On one hand the elemental detection for optical emission spectrometry is taking benefit of the dissociative character and on the other hand, DBDs can be applied as excellent as soft ionization sources for mass spectrometry.

Acknowledgements

The financial support by the Ministerium für Innovation, Wissenschaft, Forschung und Technologie des Landes Nordrhein-Westfalen, by the Bundesministerium für Bildung und Forschung and by the Deutsche Forschungsgemeinschaft is gratefully acknowledged.

References

1 W. Siemens, *Poggendorff's Annalen der Physik und Chemie*, 1857, **102**, 66–122.
2 G. C. Lichtenberg, *Novi Commentari Societatis Regiae Scientiarum Gottingensis, Kap.*, De nova methodo naturam ac motum fluidi electrici investigandi, pp.168–180. Commentationes physicae et mathematicae classis, Joann. Christian Dieterich, Gottingae, 8, 1778.
3 K. Buss, *Electr. Eng.*, 1932, **27**, 35–37.
4 E. Warburg, *Ann. Phys.*, 1904, **13**, 464–476.
5 E. Warburg and W. Rump, *Z. Phys.*, 1925, **32**, 245–251.
6 U. Kogelschatz, B. Eliasson and W. Egli, *Pure Appl. Chem.*, 1999, **71**, 1819–1828.
7 U. Kogelschatz, B. Eliasson and M. Hirth, *Ozone: Sci. Eng.*, 1988, **10**, 367–377.
8 B. Eliasson and U. Kogelschatz, *Appl. Phys. B: Photophys. Laser Chem.*, 1988, **46**, 299–303.
9 A. Sobel, *IEEE Trans. Plasma Sci.*, 1991, **19**, 1032–1047.
10 O. Goossens, E. Dekempeneer, D. Vangeneugden, R. Van de Leest and C. Leys, *Surf. Coat. Technol.*, 2001, **142**, 474–481.
11 B. M. Penetrante, R. M. Brusasco, B. T. Merritt and G. E. Vogtlin, *Pure Appl. Chem.*, 1999, **71**, 1829–1835.
12 B. M. Penetrante, M. C. Hsiao, J. N. Bardsley, B. T. Merritt, G. E. Vogtlin, A. Kuthi, C. P. Burkhart and J. R. Bayless, *Plasma Sources Sci. Technol.*, 1997, **6**, 251–259.
13 G. Borcia, C. A. Anderson and N. M. D. Brown, *Plasma Sources Sci. Technol.*, 2003, **12**, 335–344.
14 Z. Hubicka, M. Cada, M. Sicha, A. Churpita, P. Pokorny, L. Soukup and L. Jastrabik, *Plasma Sources Sci. Technol.*, 2002, **11**, 195–202.
15 J. R. Roth, *Phys. Plasmas*, 2003, **10**, 2117–2126.
16 A. K. Srivastava, G. Prasad, P. K. Atrey and V. Kumar, *J. Appl. Phys.*, 2008, **103**, 033302.
17 J. Franzke, *Anal. Bioanal. Chem.*, 2009, **395**, 549–557.
18 C. Meyer, R. Heming, E. L. Gurevich, U. Marggraf, M. Okruss, S. Florek and J. Franzke, *J. Anal. At. Spectrom.*, 2011, **26**, 505–510.
19 M. A. Lieberman and A. J. Lichtenberg, *Principles of Plasma Discharges and Materials Processing*, John Wiley & Sons, Inc., 1994.
20 Y. P. Raizer, M. N. Shneider and N. A. Yatsenko, *Radio-Frequency Capacitive Discharges*, CRC Press, Inc., 1995.
21 Y. P. Raizer, *Gas Discharge Physics*, Springer Verlag, Berlin, 1991.
22 M. M. Turner, *J. Phys. D: Appl. Phys.*, 2009, **42**, 194008.
23 U. Kogelschatz, B. Eliasson and W. Egli, *J. Phys. IV France*, 1997, **7**, C4–C47.
24 F. Massines, N. Gherardi, N. Naude and P. Segur, *Eur. Phys. J.: Appl. Phys.*, 2009, **47**, 22805.
25 K. Kunze, M. Miclea, G. Musa, J. Franzke, C. Vadla and K. Niemax, *Spectrochim. Acta, Part B*, 2002, **57**, 137–146.
26 R. Brandenburg, Z. Navratil, J. Jansky, P. St'ahel, D. Trunec and H. E. Wagner, *J. Phys. D: Appl. Phys.*, 2009, **42**, 085208.
27 M. Miclea, K. Kunze, G. Musa, J. Franzke and K. Niemax, *Spectrochim. Acta, Part B*, 2001, **56**, 37–43.
28 K. Kunze, A. Zybin, J. Koch, J. Franzke, A. Miclea and K. Niemax, *Spectrochim. Acta, Part A*, 2004, **60**, 3393–3401.
29 Z. L. Zhu, S. C. Zhang, J. H. Xue and X. R. Zhang, *Spectrochim. Acta, Part B*, 2006, **61**, 916–921.
30 Z. L. Zhu, S. C. Zhang, Y. Lv and X. R. Zhang, *Anal. Chem.*, 2006, **78**, 865–872.
31 Z. L. Zhu, Z. F. Liu, H. T. Zheng and S. H. Hu, *J. Anal. At. Spectrom.*, 2010, **25**, 697–703.
32 Z. L. Zhu, J. X. Liu, S. C. Zhang, X. Na and X. R. Zhang, *Anal. Chim. Acta*, 2008, **607**, 136–141.
33 Z. L. Zhu, J. X. Liu, S. C. Zhang, X. Na and X. R. Zhang, *Spectrochim. Acta, Part B*, 2008, **63**, 431–436.
34 Z. L. Zhu, G. C. Y. Chan, S. J. Ray, X. R. Zhang and G. M. Hieftje, *Anal. Chem.*, 2008, **80**, 8622–8627.
35 Y. L. Yu, Z. Du, M. L. Chen and J. H. Wang, *Angew. Chem., Int. Ed.*, 2008, **47**, 7909–7912.
36 M. Puanngam, S. I. Ohira, F. Unob, J. H. Wang and P. K. Dasgupta, *Talanta*, 2010, **81**, 1109–1115.
37 Y. L. Yu, Z. Du, M. L. Chen and J. H. Wang, *J. Anal. At. Spectrom.*, 2008, **23**, 493–499.
38 R. Guchardi and P. C. Hauser, *J. Anal. At. Spectrom.*, 2004, **19**, 945–949.
39 R. Guchardi and P. C. Hauser, *J. Anal. At. Spectrom.*, 2003, **18**, 1056–1059.
40 R. Guchardi and P. C. Hauser, *Analyst*, 2004, **129**, 347–351.
41 R. Guchardi and P. C. Hauser, *J. Chromatogr., A*, 2004, **1033**, 333–338.
42 G. Jenkins and A. Manz, *J. Micromech. Microeng.*, 2002, **12**, N19–N22.
43 M. R. Webb, F. J. Andrade and G. M. Hieftje, *Anal. Chem.*, 2007, **79**, 7899–7905.

44 M. R. Webb, F. J. Andrade and G. M. Hieftje, *Anal. Chem.*, 2007, **79**, 7807–7812.
45 S. Tombrink, S. Muller, R. Heming, A. Michels, P. Lampen and J. Franzke, *Anal. Bioanal. Chem.*, 2010, **397**, 2917–2922.
46 R. Heming, A. Michels, S. B. Olenici, S. Tombrink and J. Franzke, *Anal. Bioanal. Chem.*, 2009, **395**, 611–618.
47 K. W. Jo, M. G. Kim, S. M. Shin and J. H. Lee, *Appl. Phys. Lett.*, 2008, **92**, 011503.
48 N. Na, M. X. Zhao, S. C. Zhang, C. D. Yang and X. R. Zhang, *J. Am. Soc. Mass Spectrom.*, 2007, **18**, 1859–1862.
49 N. Na, C. Zhang, M. X. Zhao, S. C. Zhang, C. D. Yang, X. Fang and X. R. Zhang, *J. Mass Spectrom.*, 2007, **42**, 1079–1085.
50 J. D. Harper, N. A. Charipar, C. C. Mulligan, X. R. Zhang, R. G. Cooks and Z. Ouyang, *Anal. Chem.*, 2008, **80**, 9097–9104.
51 Y. Zhang, X. X. Ma, S. C. Zhang, C. D. Yang, Z. Ouyang and X. R. Zhang, *Analyst*, 2009, **134**, 176–181.
52 Y. Y. Liu, Z. Q. Lin, S. C. Zhang, C. D. Yang and X. R. Zhang, *Anal. Bioanal. Chem.*, 2009, **395**, 591–599.
53 X. X. Ma, S. C. Zhang, Z. Q. Lin, Y. Y. Liu, Z. Xing, C. D. Yang and X. R. Zhang, *Analyst*, 2009, **134**, 1863–1867.
54 M. R. Almasian, C. D. Yang, Z. Xing, S. C. Zhang and X. R. Zhang, *Rapid Commun. Mass Spectrom.*, 2010, **24**, 742–748.
55 Z. Xing, J. A. Wang, G. J. Han, B. Kuermaiti, S. C. Zhang and X. R. Zhang, *Anal. Chem.*, 2010, **82**, 5872–5877.
56 G. M. Huang, O. Y. Zheng and R. G. Cooks, *Chem. Commun.*, 2009, 556–558.
57 G. M. Huang, W. Xu, M. A. Visbal-Onufrak, Z. Ouyang and R. G. Cooks, *Analyst*, 2010, **135**, 705–711.
58 L. Gao, Q. Y. Song, G. E. Patterson, R. G. Cooks and Z. Ouyang, *Anal. Chem.*, 2006, **78**, 5994–6002.
59 J. F. Garcia-Reyes, F. Mazzotti, J. D. Harper, N. A. Charipar, S. Oradu, Z. Ouyang, G. Sindona and R. G. Cooks, *Rapid Commun. Mass Spectrom.*, 2009, **23**, 3492.
60 A. U. Jackson, J. F. Garcia-Reyes, J. D. Harper, J. S. Wiley, A. Molina-Diaz, Z. Ouyang and R. G. Cooks, *Analyst*, 2010, **135**, 927–933.
61 Y. Xia, Z. Ouyang and R. G. Cooks, *Angew. Chem., Int. Ed.*, 2008, **47**, 8646–8649.
62 N. Na, Y. Xia, Z. L. Zhu, X. R. Zhang and R. G. Cooks, *Angew. Chem., Int. Ed.*, 2009, **48**, 2017–2019.
63 A. Michels, S. Tombrink, W. Vautz, M. Miclea and J. Franzke, *Spectrochim. Acta, Part B*, 2007, **62**, 1208–1215.
64 W. Vautz, A. Michels and J. Franzke, *Anal. Bioanal. Chem.*, 2008, **391**, 2609–2615.
65 H. Hayen, A. Michels and J. Franzke, *Anal. Chem.*, 2009, **81**, 10239–10245.
66 S. B. Olenici-Craciunescu, A. Michels, C. Meyer, R. Heming, S. Tombrink, W. Vautz and J. Franzke, *Spectrochim. Acta, Part B*, 2009, **64**, 1253–1258.
67 M. Schilling, D. Janasek and J. Franzke, *Anal. Bioanal. Chem.*, 2008, **391**, 555–561.
68 A. K. Stark, M. Schilling, D. Janasek and J. Franzke, *Anal. Bioanal. Chem.*, 2010, **397**, 1767–1772.
69 A. K. Stark, C. Meyer, T. Kraehling, G. Jestel, U. Marggraf, M. Schilling, D. Janasek and J. Franzke, *Anal. Bioanal. Chem.*, 2011, 561.
70 Y. H. He, Y. Lv, Y. M. Li, H. R. Tang, L. Tang, X. Wu and X. D. Hou, *Anal. Chem.*, 2007, **79**, 4674–4680.
71 Y. M. Li, J. Hu, L. Tang, Y. H. He, X. Wu, X. D. Hou and Y. Lv, *J. Chromatogr., A*, 2008, **1192**, 194–197.

